J. Physiol. (1976), **259**, *pp.* 251–282
With 2 plates and 14 text-figures
Printed in Great Britain

FUNCTIONAL CHARACTERISTICS OF LATERAL INTERACTIONS BETWEEN RODS IN THE RETINA OF THE SNAPPING TURTLE

BY D. R. COPENHAGEN AND W. G. OWEN

From the Department of Physiology, University of California, San Francisco, California 94143, U.S.A.

(*Received 30 April 1975*)

SUMMARY

1. Intracellular recordings were made of the slow hyperpolarizing light responses of single rods in the retina of the snapping turtle. Physiological criteria used to identify rods were verified by intracellular injections of Procion Yellow.

2. The amplitudes of the responses elicited by fixed intensity flashes increased as the stimulus was enlarged to a diameter of 300 μm. Scattered light was found incapable of accounting for this effect, which must result from summative interaction of rods with neighbouring receptors. Effects of summative interaction were observed even at stimulus intensities that produced maximal responses. Enlarging the diameter of the higher intensity stimuli from 100 to 300 μm increased the peak response amplitude by almost 50 %; it also produced a distinct initial peak of the response which we term the overshoot. The amplitude of this overshoot was graded with stimulus size.

3. Complete intensity–response relationships were determined using stimulus diameters of 100 and 750 μm for each rod. With the smaller stimulus the intensity response range was 4·5 log units, and with the larger stimulus this was increased to 5·0 log units. For intensities below about 60 quanta/μm^2 per flash (514 nm) the amplitudes elicited by the large stimulus followed a sigmoid-shaped curve. However, at higher intensities an additional lobe appeared on the intensity–response relationship. The appearance of this lobe correlated with the emergence of the overshoot on the response wave form.

4. Determinations of rod flash sensitivity (mV per quantum per μm^2) showed that it increased with stimulus size up to a stimulus diameter of about 300 μm. With diameters between 50 and 150 μm, a linear relationship existed between the flash sensitivity and stimulus area. Absolute quantal sensitivities increased with stimulus area by a factor of 26, from

a value of 28 μV per photoisomerization per rod with a stimulus 25 μm in diameter, to 720 μV per photoisomerization per rod with a stimulus 300 μm in diameter.

5. By comparison, red-sensitive cones showed increased sensitivity as a function of stimulus size only up to a stimulus diameter of 120 μm. Their over-all sensitivity was lower than that of rods and proved linear with stimulus diameter rather than with stimulus area.

6. Simultaneous recordings were made from rod–cone pairs to determine whether the overshoot, and hence the lobe on the amplitude–intensity function, could result from a cone input to the rod response. The time course of the cone response proved much too rapid to fit the overshoot of the rod response.

7. The spectral sensitivity of the dark-adapted rod response closely followed the difference spectrum of the rod photopigment for wave-lengths > 450 nm. This was true throughout the intensity range of the response, including low intensities where response averaging was necessary.

8. At low response amplitudes (~ 1 mV), about 70% of the 40 rods tested showed responses to long wave-length stimuli consisting of two components. The smaller shorter latency component was found by its spectral response and its time course to result from excitation of cones. Even at the low stimulus intensities which revealed the short-latency component, our results indicate that cones make no significant contribution to the peak amplitude of the response.

9. At higher stimulus intensities the rod component became larger in amplitude and shorter in latency, the cone component becoming relatively so small as to be completely masked. Under these conditions the responses to different spectral stimuli were superimposable, provided that relative intensities were adjusted for equal quantum catches by the rod photopigment. Hence the rod responses were spectrally univariant at all but the lowest stimulus intensities.

10. It is concluded that the summative interaction observed in this work is almost exclusively from rod to rod. Any given rod sums signals originating from other rods within a radius of about 150 μm. This summative interaction affects the sensitivity, maximum amplitude and wave form of the light response.

11. By comparison with recent reports by Schwartz (1975*a*, *b*), our rod quantal sensitivities are consistently higher by a factor of 4–5 and we find no cone contribution to the peak amplitude of the response. Evidence is presented that these differences result from our retinas being more fully dark-adapted. Also, our rod receptive fields had only three-fifths the diameter reported by Schwartz; possible explanations of this difference are suggested.

12. Procion Yellow injections revealed fine processes extending laterally for up to 35 μm from the rod's synaptic terminal in the outer plexiform layer. These processes exhibit *en passage* and terminal swellings. A possible pathway is thus suggested for summative interaction between distant rods.

INTRODUCTION

At the outset of this work it was well known that cones in the retina of the red-eared turtle, *Pseudemys scripta elegans*, do not respond independently but are strongly influenced by interactions with neighbouring cones (Baylor, Fuortes & O'Bryan, 1971). Recordings of massed receptor potentials in cat and monkey had indicated that receptor interactions also influence the latency near threshold, and the wave form, of rod receptor potentials (Arden & Brown, 1965; Brown, Watanabe & Murakami, 1965). In this work we undertook a systematic study of receptor interactions that influence the intracellularly recorded responses of single rods. As experimental animal we chose the snapping turtle, based upon a histological comparison of its rods and cones with those of other animals. The rod responses proved to be influenced markedly by summative interactions with other receptors. Such interactions have now been reported independently in the snapping turtle by Schwartz (1973, 1975*a*, *b*), and in *Bufo marinus* by Fain (1975).

The specific purposes of our work have been (1) to demonstrate clearly the summative interactions between rods, (2) to determine which photoreceptor classes are responsible for these interactions, (3) to measure the distance over which these interactions occur, and (4) to determine the functional consequences of such interactions upon the rod's response. Our findings on these subjects have been described briefly elsewhere (Copenhagen & Owen, 1974) and are given in detail in this paper.

METHODS

Preparation and recording

Experiments were performed on isolated eyecups of snapping turtles. The common snapping turtle, *Chelydra serpentina*, and the Florida snapping turtle, *Chelydra osceola*, were both used with identical results. The snapping turtle was chosen following a histological survey of many species reputed to have large photoreceptors. Its rods and cones both proved to have sufficient size and population density to be favourable for intracellular recording. Animals with carapace lengths of 10–14 in. were found most suitable.

The animal was decapitated and the head immediately pithed. The eyes were enucleated, prepared and mounted using techniques similar to those of Baylor & Hodgkin (1973). The eyecup preparation was maintained at room temperature (20° C) in a flow of moist O_2, either pure or mixed with 5% CO_2, in a recording

chamber shown in Text-fig 1*A*. Under these conditions the retinae remained viable for 4–6 hr.

Micro-electrodes were drawn on a modified Livingston electrode puller and had resistances, as measured in the vitreous humour with a D.C. current pulse, of 300–

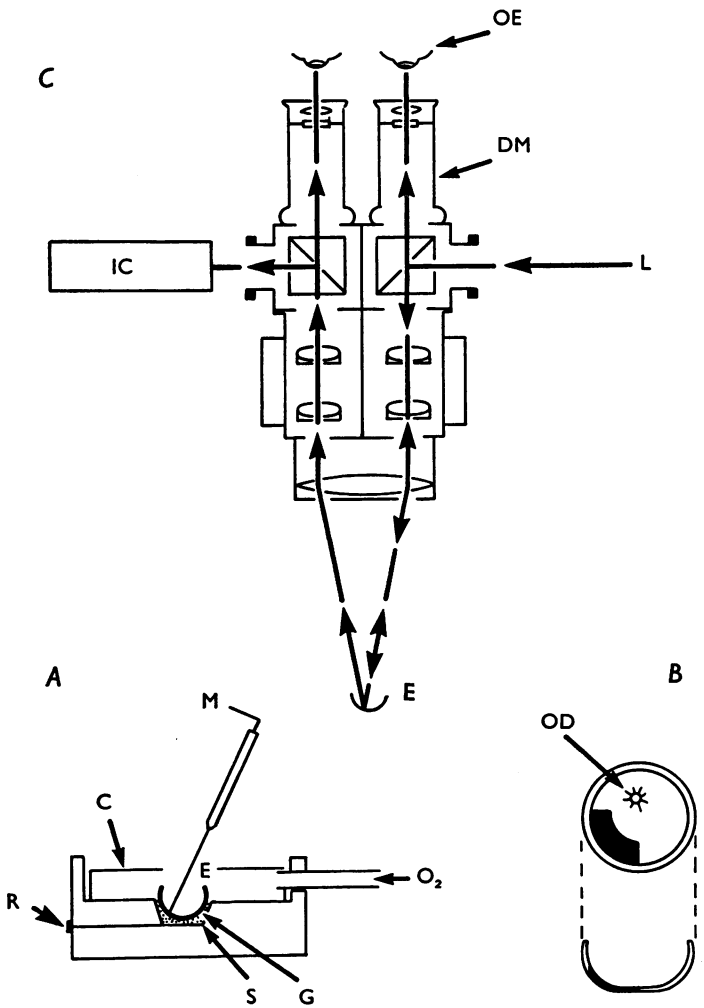

Text-fig. 1. *A*, diagram of chamber to illustrate manner in which responses were recorded. E, eyecup; G, Ringer-based gelatin; S, Ag/AgCl reference electrode; R, reference electrode terminal; C, cover; M, micro-electrode.

B, diagram of eyecup to illustrate region in which responses were recorded (dark area). OD, optic disk.

C, diagram to illustrate the manner in which light was delivered to the preparation. L, collimated light from the photostimulator; DM, Zeiss dissection microscope; E, eyecup; IC, infra-red image converter; OE, observer's eye.

400 MΩ. They were advanced into the retina from the vitreal side at an angle of about 35° from the perpendicular. All penetrations were made in the peripheral retina on the side opposite from the optic disk (see Text-fig. 1*B*). Intracellular potentials were led by an Ag/AgCl wire to a high impedance preamplifier (Winston model 1090). Amplification was direct coupled, the measured time constant of the recording system being 10 msec with a 500 MΩ electrode resistance. When necessary, weak responses were averaged using a Mnemotron computer of average transients (CAT, Model 400B).

Light stimulation

Light stimuli were delivered through a Zeiss stereo dissecting microscope, as shown in Text-fig. 1*C*. Collimated light from the optical stimulator (shown schematically in Text-fig. 2) entered an otherwise light-tight Faraday cage, and was focused on the preparation by the microscope, which provided a long working distance of 4 in. The numerical aperture of the system was 0·05. An infra-red image converter (U.S. Navy surplus) looked through the left-eye optics and could be used during experiments to view the preparation, electrode and stimulus, allowing adjustments of their relative positions without light-adapting the retina. The stimulus was also

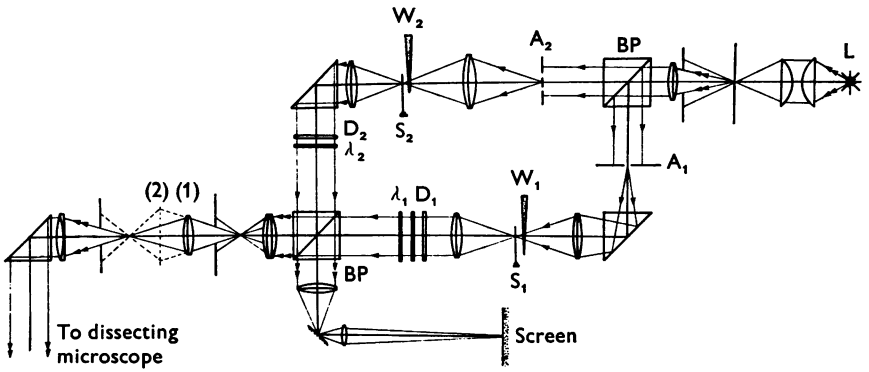

Text-fig. 2. Schematic representation of optical stimulator (not to scale). L, primary light source; BP, prism beamsplitters; A_1, A_2, stimulus apertures; W_1, W_2, neutral density wedges; S_1, S_2, electromagnetic shutters; D_1, D_2, neutral density filters; λ_1, λ_2, narrow bandwidth interference filters. Stimuli could be viewed on a screen outside the light-tight cage for alignment of the two stimulus beams.

focused roughly in this way, fine focusing being attained by viewing brief flashes of white light directly through the microscope. Stimuli could be centred quickly upon an impaled receptor using a simple procedure. The image of a narrow slit, flashed on to the retina, was moved to the position where it elicited a response of maximum amplitude. Equal segments of the slit image were then exposed in turn, and a small circular stimulus was substituted for the segment that elicited the largest response. Finally, small adjustments were made of the stimulus position to assure accurate centring upon the impaled receptor.

The optical stimulator permitted stimuli ranging in diameter from 4 μm to more than 3 mm to be presented to the retina. The stimuli consisted of two light patterns whose configurations, sizes, positions, durations, times of presentation, colour and intensities were independently adjustable.

Stimulus calibration

Measurements of stimulus irradiance in the plane of the retina were made using an irradiance meter (United Detector Technology, Opto-meter, model 40-A). With the 514 nm interference filter in the stimulus beam the maximum stimulus irradiance was 292,000 quanta sec^{-1} μm^{-2}. Thus, in a 20 msec flash of 514 nm light, a maximum of 5840 quanta could be delivered to each square micrometre of retina beneath the stimulus. The relative energy transmitted by each of the spectral interference filters was also determined.

The distribution of energy across each of the smaller stimuli was measured using a 5 μm diameter aperture placed in front of a photomultiplier as described by Baylor & Hodgkin (1973). Thus stimulus diameters were accurately known.

The 'strength' of incident illumination is most correctly referred to as its *irradiance*. The term *intensity* is often used synonymously, however, and will be used throughout the remainder of this paper when referring to the irradiance of the stimulus upon the retina.

The effective collecting area of a single rod

Stimulus intensities are given in quanta sec^{-1} μm^{-2}. In order to calculate the number of visual pigment molecules that are bleached in each rod, we must have an estimate of the rod's effective collecting area. From measurements made on both histological sections and whole-mounted retinae, we found the rod inner segments to have an average diameter of about 11 μm (see Pl. 1*A*). Hence their cross-sectional area will be about 100 μm^2. O'Brien (1951) calculated from physical models that only about 0·5 of the light within an inner segment will be funnelled into the outer segment. Our analysis of the optical properties of the snapping turtle rod, using values of the refractive indices given by Sidman (1957), is consistent with that estimate. The specific axial density of rod pigment is about 0·014/μm (Liebman, 1972). The outer segments of snapping turtle rods are about 18 μm long. Thus the total axial density of the pigment will be 0·25, so that 0·44 of the photons entering the outer segment will be absorbed. Dartnall (1972) gives the quantum efficiency of bleaching as 0·62. Hence, the effective collecting area of the snapping turtle rod is about

$$100 \times 0{\cdot}5 \times 0{\cdot}44 \times 0{\cdot}62 \simeq 13{\cdot}6\ \mu m^2.$$

A brief, flashed stimulus delivering n quanta/μm^2 to the retina will therefore bleach $n \times 13{\cdot}6$ visual pigment molecules in each rod outer segment.

Injection of Procion Yellow dye into impaled rods

The micro-electrodes were filled with a 4 % solution, weight by volume, of Procion Yellow M4R dissolved in 0·15 M-KCl. The dye was injected iontophoretically by passing a continuous negative current of 0·5–2·0 nA for 2–5 min. At least 1 hr elapsed between injection of the dye and fixation of the retina to allow for diffusion throughout the cell.

The retinas were fixed overnight in paraformaldehyde (pH 4·0) before being dehydrated with acetone. The regions containing marked cells were cut out and embedded in Epon. Serial sections were then cut perpendicular to the retinal surface at a thickness of 15 μm, mounted with a low-fluorescence mounting medium, and scanned under a Zeiss fluorescence microscope. Successfully marked and recovered cells were photographed with Kodak High Speed Ektachrome film.

Experimental controls

All experiments were conducted on well dark-adapted retinae. Because of the slowness of rods in recovering from effects of previous stimulation, special precautions

were taken to ensure that each stimulus was delivered to a fully dark-adapted cell. We found that even with the weakest stimuli the recovery of rod sensitivity, response amplitude and wave form might require 8–10 sec. Following the most intense stimulus flashes the rod response required several minutes to recover full dark-adaptation. In each experiment we determined the time required for recovery of dark adaptation, and adjusted the interval between stimuli to more than allow for full recovery of dark adaptation.

In experiments on isolated preparations, and with intracellular recording, it is especially important to monitor the normality of the cell from which recordings are made. A standard stimulus was thus repeated at intervals during experiments, and if the response showed any significant sign of deterioration, the data were discarded.

RESULTS

The evaluation of scattered light

In any study of receptor interaction, particularly where the interaction may be summative, it is important to make some estimate of the extent to which light scatter can affect the results. Previous authors have sought to do this by assuming light to be scattered within the retina according to a Gaussian scattering distribution (Baylor, Fuortes & O'Bryan, 1971; Schwartz, 1973). The retina, however, consists of a suspension of transparent cells whose dimensions are considerably larger than the wavelength of light. An assumption of Gaussian scattering is inappropriate for such a case. The form of the scattered intensity function can be obtained by applying the rigorous scattering theory of Mie (1908) though considerable computation is necessary. Hodkinson & Greenleaves (1963) developed an approximation to the Mie theory which is less cumbersome to use. Our use of their method in deriving the scattered intensity function of the retina is described in the Appendix. The applicability of a theoretically derived function to our practical case, however, can only be determined by comparison with a direct measure of the quantity of light delivered to the receptors. A direct measurement can be obtained by observing the response of a single photoreceptor *if* that receptor is known to be free from interactions with other receptors.

Data from an isolated cone in an eyecup preparation of the red-eared turtle, *Pseudemys scripta elegans*, were published by Baylor & Hodgkin (1973). When we perform the convolution of the intensity distribution of their stimulus (Baylor & Hodgkin, 1973, fig. 2) with our calculated scattered intensity function (Text-fig. 12), the distribution of light 'seen' by their isolated cone is satisfactorily predicted (Text-fig. 13). In view of the similarity between the retinae of the red-eared turtle and the snapping turtle we believe the theoretically derived function to be a realistic description of light scatter in either retina.

Applying this function to our present experiments, we calculate that

increasing the diameter of a fixed intensity stimulus from 25 to 250 μm will produce only a 2·4-fold increase in the light falling upon the impaled receptor (see Text-fig. 13). Increasing stimulus diameter beyond 250 μm should not alter the light falling on the receptor. Thus the effect of light scattering upon the rod response will be small. The large variations in response amplitude (Text-fig. 3) and flash sensitivity (Text-fig. 8) that we observe as we vary stimulus diameter must result primarily from lateral summative interactions.

Response characteristics of photoreceptors

Receptors were usually penetrated at a depth of about 180 μm, which was consistent with the depth of the photoreceptor layer in histological sections (see Pl. 1*B*). Penetration was aided by applying about 30 mV of a 60 Hz signal across the electrode tip. After penetration the stimulus was carefully centred upon the impaled cell, as described in the Methods. The cell was then identified by examining its receptive field size, spectral sensitivity, adaptation characteristics and response wave form.

Photoreceptors were readily distinguished from horizontal cells, since the receptive fields of receptors did not exceed 300 μm in diameter, whereas those of horizontal cells were never less than 500 μm in diameter and were usually much larger.

The response characteristics of snapping turtle cones were identical with those of the red-eared turtle, *Pseudemys scripta elegans* (Baylor & Fuortes, 1970; Baylor *et al.* 1971; Baylor & Hodgkin, 1973). Following exposure to even the brightest flashes, the cones readapted readily, 15–20 sec being generally sufficient to allow complete recovery of sensitivity.

Penetration of a rod was signalled by the appearance of a resting potential, usually of between -30 and -40 mV, the median value being -34 mV. Long duration, bright spots of light produced a rapid hyperpolarization that peaked during the stimulus exposure and then returned slowly towards the resting potential. At stimulus termination there was no obvious change in the rate of this return, the cell remaining hyperpolarized for many seconds. The amplitude of the saturated response elicited by large stimuli was about 28 mV below the resting potential. The sensitivity of the rods was almost two log units greater than that of cones when large stimuli (> 300 μm diameter) were used. Following exposure to a bright flash of light, the rods readapted so slowly that several minutes had to elapse before recovery of sensitivity was complete. The rod spectral sensitivity peaked at about 520 nm (see Text-fig. 9), which is consistent with the absorption maximum of the snapping turtle's rod visual pigment (Liebman, 1972).

Cells stained with Procion Yellow

Procion Yellow dye was injected into nine cells identified as rods on the basis of their response characteristics. Four were subsequently recovered and examined under the fluorescence microscope. In the two cells shown in Pl. 2*A*, and also in a third not photographed, the dye filled fine basal processes which extended from the synaptic terminals. The processes of two cells extended into adjacent histological sections. Pl. 2*B* shows camera lucida tracings of the basal processes of these three cells made from all the sections which contained them. Between 5 and 9 processes were seen to extend laterally from each cell for distances up to 35 μm. Most of them made a slight proximal excursion into the outer plexiform layer, though one was noted to terminate at the level of the receptor nuclei. A majority of the processes possessed terminal swellings ranging in diameter from 0·5 to 1·0 μm and in some cases *en passage* swellings were also seen.

The dye-marked cells were compared with snapping turtle receptors stained with the Golgi method by H. Leeper & W. K. Stell (personal communication). They found that the cone nucleus is connected to its synaptic terminal by a thin fibre, whereas the rod nucleus communicates with its synaptic terminal via a thick stem. The cone synaptic terminal is rounded and sends out fine basal processes which extend laterally 10–40 μm. The rod synaptic terminal is broad and flat and also sends out long basal processes extending up to about 40 μm from their origin. Snapping turtle rods as described by Leeper & Stell are thus morphologically similar to the rods of the red-eared turtle, *Pseudemys scripta elegans* (Lasansky, 1971). All our dye-marked cells clearly correspond in structure with Golgi-stained rods. We are thus confident in identifying rod receptor potentials on the basis of their response characteristics, which have been validated by histological methods.

Spatial dependence of rod response amplitude

The effects of increasing stimulus diameter upon rod response amplitude are shown in Text-fig. 3. Circular flashes of fixed intensity ranging in diameter from 25 to 500 μm were presented to the impaled rod and the peak amplitudes of the elicited responses were measured. Data from four rods are plotted in Text-fig. 3, where all amplitudes have been normalized against the value obtained with a stimulus 500 μm in diameter. At the intensities we used the smallest stimuli elicited responses of 2–3 mV, while the largest ones yielded responses of 12·3–15·2 mV. In each rod the response amplitude for the largest stimulus was only about half the rod's maximum response amplitude.

Our analysis of scattered light implies that enlarging the stimulus beyond

25 μm in diameter could increase the stimulus intensity at the receptor by a factor no larger than 2·4 (see Text-fig. 14). An increase of that magnitude would cause the response amplitude to increase by a factor of less than 2·0. Experimentally, however, we found that enlarging the stimulus from 25 to 300 μm in diameter produced about a fivefold increase in response amplitude. Beyond 300 μm the response amplitude was independent of stimulus diameter. These results strongly suggest that the responses of neighbouring receptors can contribute to the amplitude of the response recorded in the impaled rod.

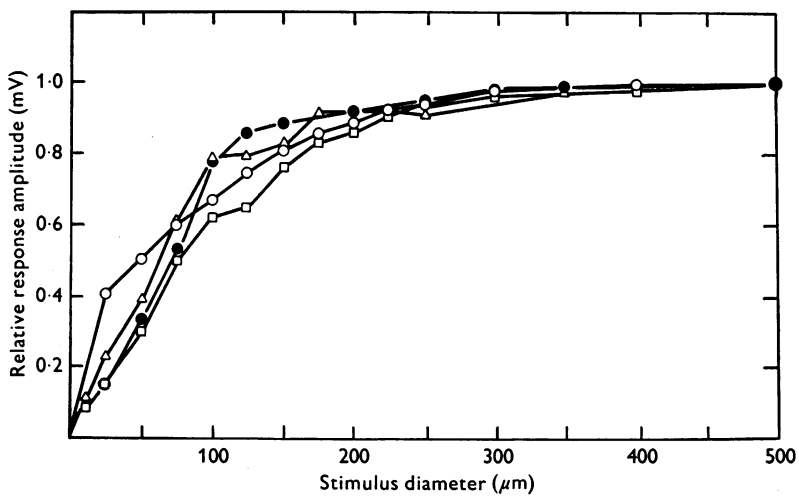

Text-fig. 3. The relative variation in peak amplitude of the rod response as a function of stimulus diameter. Stimuli were flashes of white light, 200 msec in duration, at an intensity approximately 3 log units below saturation. For each of four rods, data are plotted as fractions of the amplitude of the response elicited by the stimulus 500 μm in diameter.

There are differences between our results in Text-fig. 3, and those of Schwartz (1973, 1975*a*) in relation to the size of the rod's summation area which we define as the minimum stimulus area required to elicit the rod's full-field response. We consistently found the diameter of this area to be 300 μm, while values of 400 and 500 μm have been reported by Schwartz (1973, 1975*a*, respectively). Since the diameter over which this summative interaction occurs is one of the important characteristics of rods, it will be discussed later in this paper.

Spatial dependence of the rod's maximum response amplitude

With stimuli less than 300 μm in diameter, enlarging the stimulus caused a decreased time-to-peak, as well as an increased peak amplitude. These effects occurred at stimulus intensities throughout the rod's response range. Of special interest is that these effects occurred even at stimulus intensities that elicited rod responses of maximal amplitude. To demonstrate this a control stimulus of 100 μm diameter was first delivered at an intensity sufficient to elicit a maximal response. The response to this control stimulus reached a peak amplitude of 20 mV at 480 msec after the onset of the stimulus, as shown in Text-fig. 4*A*. When the stimulus diameter was increased to 750 μm, the response amplitude increased to 29 mV. Though the latency remained unchanged at 40 msec, the time-to-peak was shortened to 190 msec and recovery toward the base line was slower. The difference in the light intensities scattered on to the impaled rod from each of these stimuli was calculated to be less than 0·05 log units. Increasing the intensity of either stimulus produced no increase of response amplitude. Hence Text-fig. 4*A* demonstrates that stimulation of neighbouring receptors markedly alters both the time course of the rod response, and its maximum amplitude.

The increase in peak amplitude and decrease in time-to-peak of the maximal response varied in a graded manner as the stimulus was enlarged up to a diameter of about 300 μm. Text-fig. 4*B* shows responses elicited by stimuli of five different diameters ranging from 75 to 250 μm. The response to each stimulus diameter was maximal, because increasing the stimulus intensity produced no increase in response amplitude. The increase in response amplitude that occurred as the stimulus was enlarged resulted from the development of an initial peak on the wave form, and the magnitude of this peak clearly depended upon the extent to which neighbouring receptors were stimulated. Since the initial peak resembles the 'overshoot' of an underdamped resonant system, it will be referred to as an overshoot in the remainder of this paper. Similar overshoots have been observed in rod responses of the toad, *Bufo marinus* (Brown & Pinto, 1974), and the frog, *Rana catesbeiana* (Coles & Yamane, 1975).

Amplitude–intensity characteristics of the rod's response

The dependence of the rod's response characteristics upon stimulus size was examined in greater detail by determining the relation between peak response amplitude and stimulus intensity with stimuli 100 and 750 μm in diameter. Owing to differences in quantal sensitivity between rods, it is important that the complete relation be measured with both stimulus sizes on each rod. As described in the Methods, procedures were employed

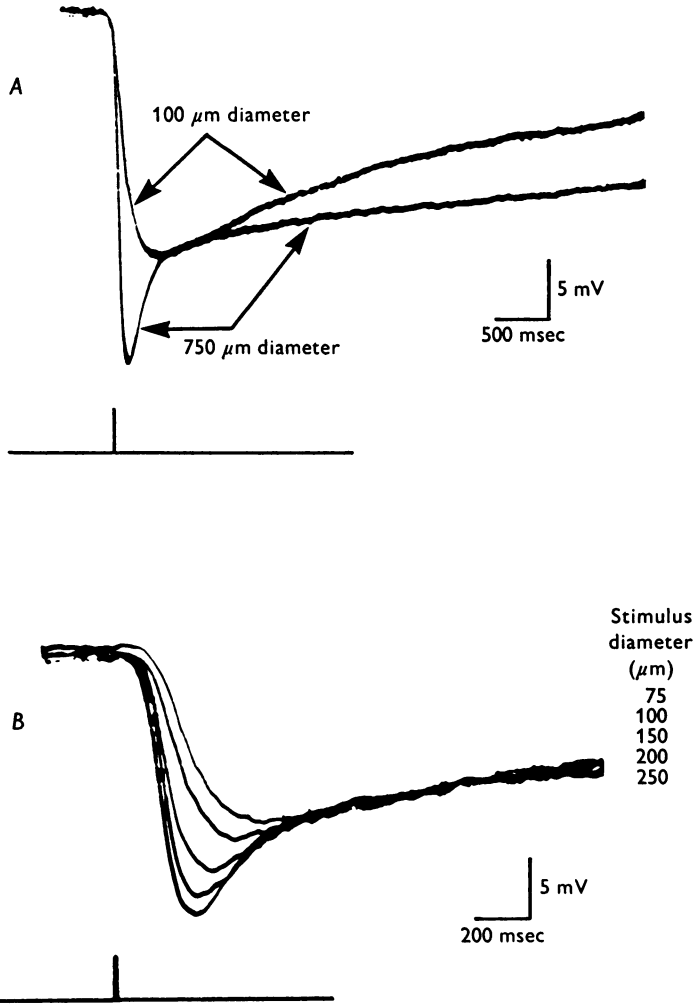

Text-fig. 4. Responses to centred stimulus flashes of saturating intensity and different diameter. Stimulus intensities were constant, about 0·5 log units above that at which the responses saturated. In *A*, 20 msec flashes of 514 nm light were presented having diameters of 100 and 750 μm. Increasing stimulus diameter resulted in a more rapid hyperpolarization and an increased peak amplitude of the saturated response, owing to the emergence of an 'overshoot' on the response wave form. Following the response peak the potentials were briefly equal, after which the response to the larger stimulus returned more slowly toward the resting potential. In *B* the spatial dependence of the magnitude of the overshoot is illustrated in more detail by showing responses to stimuli ranging from 75 to 250 μm in diameter. These responses were recorded at a faster time base than those in *A*.

to assure that each response was elicited from a fully dark-adapted cell. As a result, complete data could be obtained only when the rod remained stable and healthy throughout the 1·5 hr the measurements required. Of the nine rods examined in this way, three provided complete data, which are presented in Text-fig. 5.

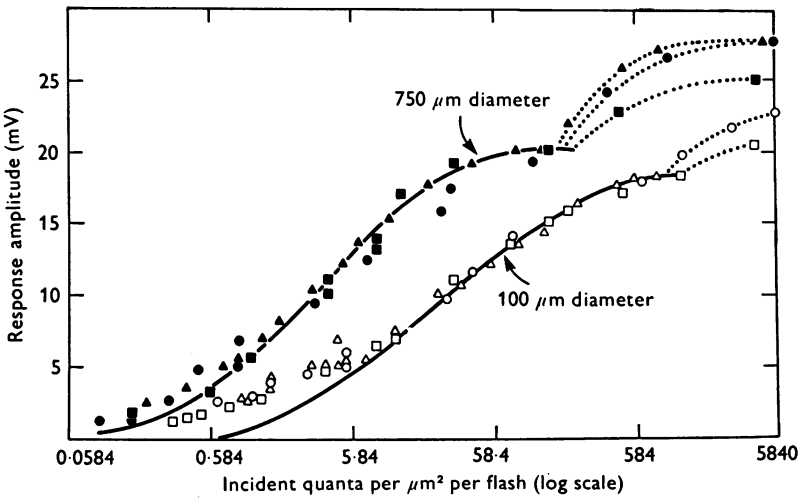

Text-fig. 5. Amplitude–intensity characteristics of the rod response measured with stimuli 100 and 750 μm in diameter. Stimuli were 20 msec flashes of 514 nm light. Peak response amplitude is plotted against the number of quanta/μm^2 delivered in each flash (logarithmic scale). Results are given for three rods, each represented by a separate symbol. Note that for each rod, complete data were obtained with both stimulus diameters. The three sets of data have been adjusted to the mean position by sliding them laterally by no more than $\pm$ 0·1 log units. The continuous curves were generated by the function $V/V_{max} = I^n/I^n + \sigma^n$, where $n = 0{\cdot}9$. For further details, see text.

The solid lines drawn through the data points represent the function:

$$\frac{V}{V_{max}} = \frac{I^n}{I^n + \sigma^n}, \tag{1}$$

where V_{max} is the maximum response amplitude and σ the intensity required to elicit a response of one-half V_{max}. This function, with $n = 1$, was first used by Naka & Rushton (1966) to describe the amplitude of fish S-potentials as a function of stimulus intensity. With the value of n varying somewhat between species, this function has also been applied to vertebrate receptor potentials under a variety of conditions (Baylor & Fuortes, 1970; Boynton & Whitten, 1970; Grabowski, Pinto & Pak, 1972; Dowling & Ripps, 1972; Fain & Dowling, 1973; Normann & Werblin, 1974; Grabowski & Pak, 1975). Our closest fit for the 100 μm data was obtained

with $n = 0{\cdot}9$, $V_{max} = 18{\cdot}5$ mV, and $\sigma = 22{\cdot}2$ quanta/μm^2. This value of σ corresponds to a stimulus intensity which produces 300 photo-isomerizations per rod. At the lower intensities the data points consistently fell above the curve defined by eqn. (1).

The continuous line through the 750 μm data is the same function with $V_{max} = 20$ mV, $n = 0{\cdot}9$ and $\sigma = 3{\cdot}1$ quanta/μm^2, which corresponds to approximately 40 photoisomerizations per rod. The data do not fit this function at the highest stimulus intensities. The responses reached an apparent maximum amplitude at around 20 mV, then increased further, finally reaching their true maximum amplitude of between 26 and 28 mV. The responses elicited by the highest stimulus intensities thus added a distinct upper lobe to the points fitted by eqn. (1).

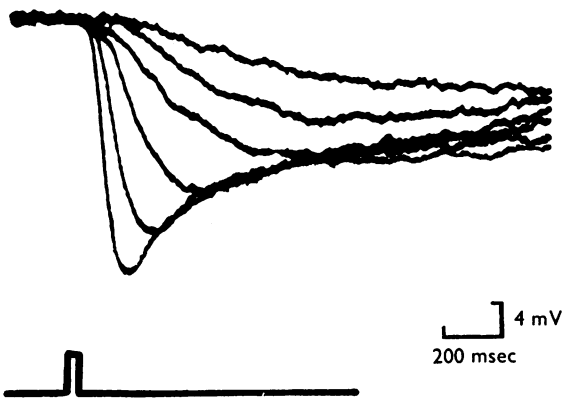

Text-fig. 6. Responses to a 750 μm diameter stimulus presented at different intensities. Flashes of 514 nm light, 20 msec in duration, were given at intensities of 1·4, 5·1, 11·4, 40·4, 176 and 625 quanta/μm^2 upon the retina. Overshoots can be observed on the responses to the three most intense stimuli.

Text-fig. 6 shows the response forms elicited by the 750 μm stimulus when presented at different intensities. With stimulus intensities up to about 40 quanta/μm^2, the responses reached peak amplitude and subsequently decayed slowly and continuously to the base line. At the higher intensities an overshoot appeared, the decay of which showed an early rapid and later slow phase. Over this same range of higher intensities the lobe of the amplitude–intensity function was seen; this lobe is thus correlated with the emergence and growth of an overshoot on the rod's response. There was little evidence of overshoot on responses to the more intense stimuli of 100 μm diameter; correspondingly, Text-fig. 5 shows only a small lobe on the amplitude–intensity function for these smaller stimuli.

The failure of eqn. (1) to describe either the data obtained at high intensities with the 750 μm diameter stimulus, or that obtained at low intensities, with the 100 μm diameter stimulus, leads us to suggest that it is an inadequate representation of processes underlying the rod response. When the value of the index, n, is unity, the approximation V_{max}/σ is often used as a measure of the flash sensitivity of a cell. In view of these findings we suggest that such an approximation is likely to be inappropriate and that a more direct method should be employed when determining the flash sensitivity of photoreceptors.

An advantage of using 100 and 750 μm stimuli in Text-fig. 5 is that they deliver virtually equal quantities of light to the impaled rod. Thus, the differences between the responses they elicit can be ascribed to spatial interactions. Clearly, by increasing the stimulus diameter at *any* intensity within the rod's response range, the response amplitude increased because of summative spatial interactions. Moreover, the rod responded over a larger voltage range and to a wider range of intensities because of these interactions. The maximum peak amplitude was increased by almost 50 % and the intensity range was extended downward by approximately 0·5 log units.

Our results indicate that the overshoot of the rod response is strongly enhanced by spatial interactions, and suggest that it may not occur at all in the absence of spatial interactions. Text-fig. 4 demonstrates that the overshoot of the maximal receptor potential is enhanced by spatial interaction under conditions where this effect cannot be mimicked by increasing stimulus intensity upon the impaled rod. Also, Text-figs. 5 and 6 together show that eqn. 1 cannot account for the lobe that the overshoot produces upon the upper portion of the rod's amplitude–intensity function. We conclude from these findings that the rod response is not generated by a single process, but that at least two processes are involved, one or both of which are influenced by spatial interactions.

One possibility is that the overshoot of the rod response, and hence the upper lobe on the amplitude–intensity function, results from an early input to the rod response from neighbouring cones. This is especially reasonable because the cone response is well known to have a shorter latency than that of rods, and to have an initial peak at high stimulus intensities. We tested this notion by using two separate electrodes to penetrate rod–cone pairs and record their responses simultaneously. Rod and cone responses were thus compared under the same conditions of stimulation, adaptation, and retinal condition. Text-fig. 7 shows typical responses from such an experiment involving a rod and a red-sensitive cone. The two cells were about 150 μm apart and were stimulated with 20 msec flashes of 633 nm light, 750 μm in diameter. The stimulus intensity

of 720 quanta/μm^2 elicited a nearly maximal rod response. When measured from stimulus onset, the time-to-peak of the cone response was 100 msec, while that of the rod response was 225 msec. By the time the rod response had reached maximum amplitude, the cone response had decayed almost halfway to the base line. This discrepancy between time courses strongly suggests that the overshoot of the rod response cannot result from an input to rods from red-sensitive cones. In single impalements, at high stimulus intensities, we find the time courses of red- and green-sensitive cone responses to be quite similar. We thus conclude that the overshoot of the rod response does not result from a cone contribution, but from spatial interaction with other rods. This conclusion is confirmed by measurements of spectral sensitivity described later in this paper.

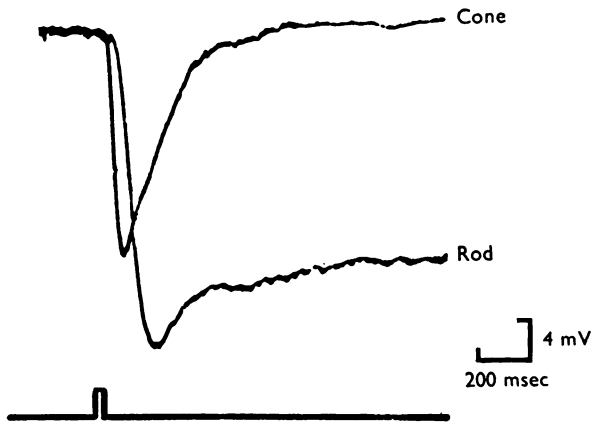

Text-fig. 7. Simultaneous responses from a rod and a red-sensitive cone impaled with independently advanced micro-electrodes. The separation between the two cells was about 150 μm, as determined by moving a small stimulus spot across the retina and noting the positions of maximal response. The stimulus was a 20 msec flash delivering 720 quanta/μm^2 at a peak wave-length of 633 nm, and having a diameter of 750 μm, which covered the receptive fields of both the rod and the cone.

Flash sensitivity as a function of stimulus size

The area over which the rod's sensitivity is spatially dependent defines its receptive field and hence the lateral extent of its interactions with other receptors. The spatial dependence of flash sensitivity was therefore studied in several rods. The flash sensitivity, S_F, is defined as the ratio of the peak hyperpolarization elicited by a dim flash to the number of photons at the optimum wave-length delivered to each square micrometre of the retina. Thus:

$$S_F = \frac{V}{I_\lambda . \Delta t}, \qquad (2)$$

where V is the peak amplitude of the response in mV, I_λ is the stimulus intensity in quanta sec^{-1} μm^{-2}, and Δt is stimulus duration in seconds. Since all these values are measured directly, no estimations are required to determine sensitivity when thus defined. The flash sensitivity of seven dark-adapted rods was studied as a function of stimulus size by eliciting responses of 1 mV criterion amplitude, using 20 msec flashes of 514 nm light. These responses fell within the linear range over which response amplitude was directly proportional to the quantity of light absorbed by the rod. The averaged data are plotted on logarithmic axes in the upper curve of Text-fig. 8.

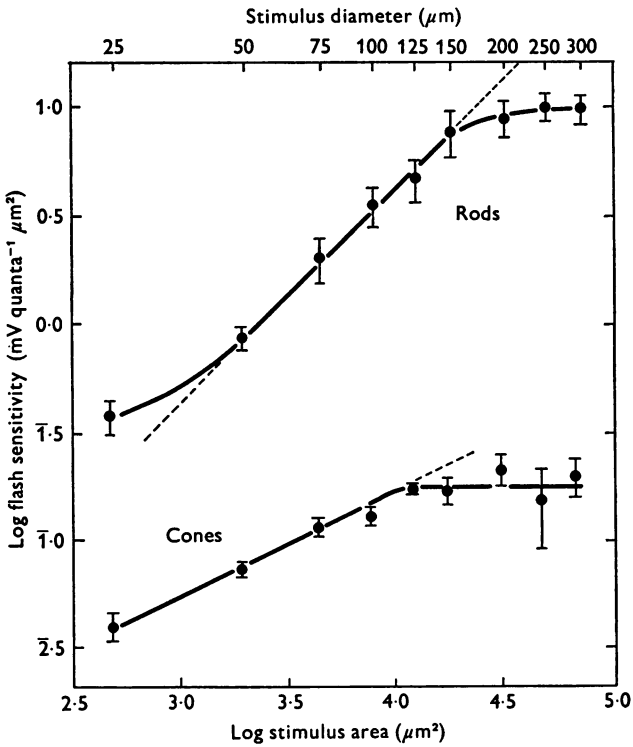

Text-fig. 8. The logarithms of the mean flash sensitivities of seven rods and five cones are plotted against the logarithm of the stimulus area. The stimuli were 20 msec flashes of 514 nm light (rods) and 618 nm light (cones), whose intensities were adjusted to elicit responses 1 mV in amplitude. For each cell and each stimulus size, the average amplitude was obtained from 5 to 10 responses. Vertical bars 1 S.E. of mean.

Using a stimulus of 25 μm diameter the mean value of sensitivity was $0{\cdot}38 \pm 0{\cdot}07$ (S.E. of mean) mV $quantum^{-1}$ μm^2. The largest value obtained with a stimulus of this diameter, however, was 0·72 mV $quantum^{-1}$ μm^2.

Using a stimulus of 300 μm diameter the mean value was $9{\cdot}8 \pm 1{\cdot}63$ (S.E. of mean) mV quantum^{-1} μm^2. It is evident that the absolute value of flash sensitivity varied somewhat between rods, but the *relative* variation in sensitivity with stimulus area was consistent from rod to rod. When this curve is compared with the variation in incident light intensity calculated for the same range of stimulus areas (Text-fig. 14), it is clear that neither the increase in flash sensitivity, nor the range of stimulus areas over which the increase occurs can be accounted for by the effects of light scatter within the retina. We thus conclude that summative interactions with neighbouring photoreceptors influence the rod response, even at the lowest of stimulus intensities.

In Text-fig. 8 the data with stimuli of 50–150 μm diameter are well fitted by the dotted straight line of slope 1·0, indicating a linear relation between flash sensitivity and stimulus area over this range. This implies that within the annulus defined by these limits, equal retinal areas make equal contributions to the sensitivity of the impaled rod.

Flash sensitivity did not increase when the stimulus was enlarged beyond 300 μm in diameter. Thus, the receptive field, as determined from these measurements, extends to a radius of 150 μm around each rod. This was also found to be true when flashes of longer duration (up to 400 msec) were used, when criterion responses of up to 10 mV were elicited, and under conditions of moderate light adaptation. Our measured value of the receptive field size is considerably smaller than the 500 μm diameter reported recently by Schwartz (1975). The difference may result from variations in rod receptive field size between different retinal areas, though Schwartz did not define the retinal region he studied. Measured receptive fields will also be too large if the stimulus is imperfectly centred upon the impaled rod.

For comparison, the mean area–sensitivity relation for five red-sensitive cones is also plotted in Text-fig. 8. The data were obtained by the same technique, the stimuli being 20 msec flashes of 618 nm light. Whereas the rod sensitivity varied with stimulus diameter up to 300 μm, the cone sensitivity varied only to a maximum diameter of 120 μm. Thus the area of a rod's receptive field is about six times that of a red cone's. Moreover, the slope of the cone function for stimuli less than 100 μm diameter is about 0·5, indicating that over this range the flash sensitivity of the red-sensitive cone is linearly related to the stimulus diameter rather than to its area. This contrasts with the finding of Baylor & Hodgkin (1973) of a slope of 1·0 over the same range for the red-sensitive cone of the red-eared turtle. This difference in slope may reflect a difference in retinal organization between the two species. The proportion of cones to rods is considerably greater in the red-eared turtle than in the snapping turtle, and the characteristics of summative cone interactions may be population dependent.

With which receptor classes do rods interact?

If the rod's response were determined by quanta absorbed in a single visual pigment, the response wave form would be independent of stimulus wave-length and could be described as spectrally *univariant*. We tested the responses of dark-adapted rods for univariance by two different criteria and found that the peak amplitude of the response was determined only by quanta absorbed in rods.

We determined the relative spectral sensitivity of dark-adapted rods by measuring the stimulus intensity required at each wave-length to elicit a response of criterion amplitude. The relative sensitivity at each wave-length was calculated using eqn. (2). Criterion amplitudes ranging from less than 1 to 25 mV were used with uniform results. Typical data are plotted on a logarithmic scale in Text-fig. 9. The circles are the mean relative sensitivities of five rods. The response criteria were peak amplitudes of 2 mV (three rods) and 3 mV (two rods). Stimuli were circular, 200 msec flashes of light, 400 μm in diameter. Large stimuli were used to ensure that all neighbouring receptors with which the rod might interact were stimulated. Mean spectral sensitivities of three additional rods are represented by the squares. Responses of less than 1 mV were elicited from these rods, and were averaged by a computer of average transients. All data were normalized against the value at 514 nm.

Liebman (1972) showed by microspectrophotometry that snapping turtle rods contain a vitamin A_2-based photopigment having an absorption maximum at 518 nm. The continuous line in Fig. 9 is the difference spectrum of such a pigment with absorption maximum at 520 nm. The nomogram from which this curve was derived (Munz & Schwanzara, 1967) is not defined at wave-lengths greater than about 620 nm. Professor F. Crescitelli, however, has generously provided unpublished measurements of the difference spectrum, made in the presence of hydroxylamine, of a purified extract of the vitamin A_2-based pigment from rods of the tadpole-stage bullfrog, *Rana catesbeiana*. These data, rescaled to an absorbance maximum at 520 nm, are plotted as the dashed line in Text-fig. 9.

The pigment curve provides a good fit to our data throughout the spectrum, including the longer wave-lengths where rod pigment absorption falls off rapidly. This close agreement between the relative spectral sensitivity of the rod and the difference spectrum of its photopigment indicates that the peak amplitude of the dark-adapted rod's response is determined only by the efficiency with which the rods themselves are stimulated. This was true for responses of 0·5 mV or greater, i.e. for stimuli intense enough to produce at least a single photoisomerization in each rod.

The spectral univariance of the rod response was tested even more

rigorously by examining the complete response wave forms to different spectral stimuli. At moderate to high intensities the responses to different spectral stimuli could be superimposed if stimulus intensities were adjusted to provide equal quantum catches by the rod photopigment. Text-fig. 10*A* shows responses to stimuli of 100 μm diameter at wave-lengths of 514 and 654 nm. Individual responses are shown on the left; when superimposed on the right the complete wave forms are seen to be identical. In Text-fig. 10*B* responses are shown to the same wave-lengths and intensities, but with the stimulus enlarged to 750 μm. Since this large stimulus more than covered the rod receptive field, it should have stimulated all receptors

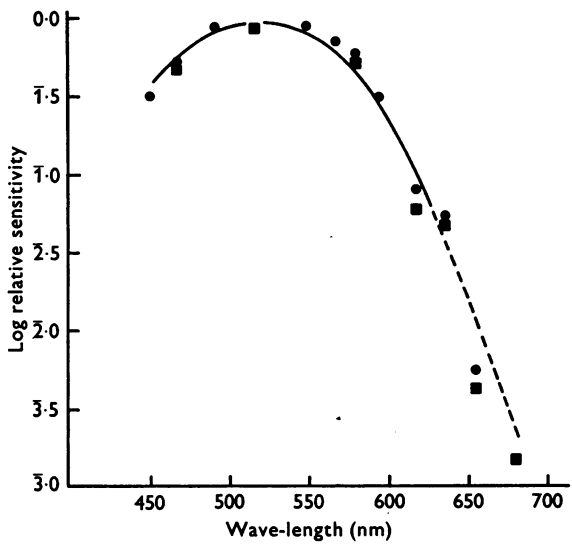

Text-fig. 9. The spectral sensitivity of the dark-adapted rod. The logarithm of the relative sensitivity is plotted as a function of stimulus wave-length. Each filled circle is the mean relative sensitivity determined from five different rods. Criterion response amplitudes of 3 mV (two rods) and 2 mV (three rods) were elicited by 200 msec stimuli of 400 μm diameter. Each square is the mean relative sensitivity for three rods in which the criterion amplitudes of < 1 mV were elicited by 20 msec stimuli of 750 μm diameter. At each wave-length, 5–10 responses were computer-averaged. The curve represents the difference spectrum for a vitamin A_2 photopigment having a peak absorbance at 520 nm.

that might interact with the impaled rod. Again the responses superimpose. Thus rod responses to relatively high stimulus intensities are spectrally univariant.

The spectral univariance of rod responses to higher intensities confirms our earlier conclusion that the overshoot does not result from a cone contribution to the rod response. Note in Text-fig. 10 that the 100 μm stimulus

does not elicit a clear overshoot, whereas the 750 μm stimulus does. If the overshoot resulted from a cone input to the rod response, the univariance observed in the responses to small stimuli should have broken down when the overshoot was introduced by using the larger stimulus. Instead, the univariance was maintained, confirming that the overshoot results from summative interaction with neighbouring rods.

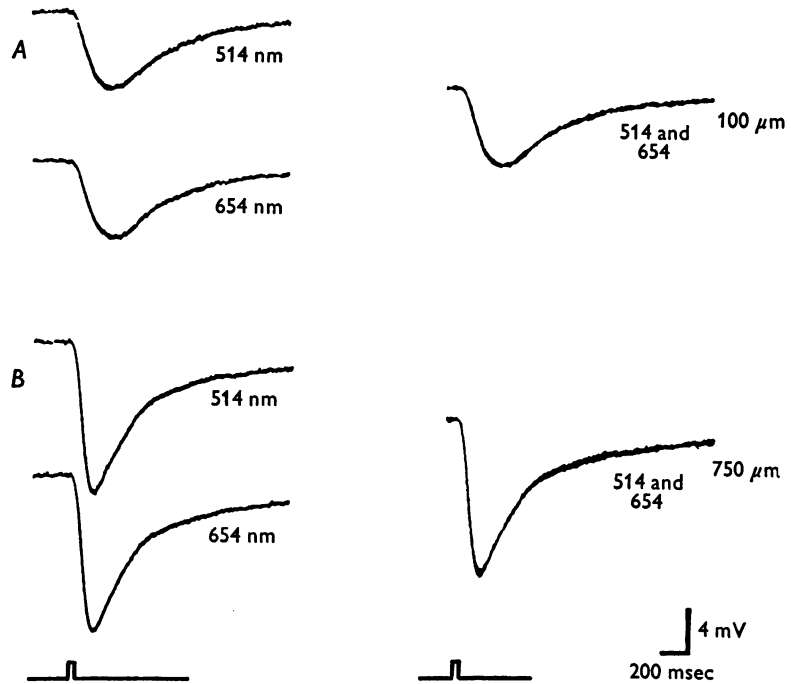

Text-fig. 10. Identical responses to stimuli of different wave-lengths that are matched for equal quantum catches by the rod photopigment. *A*, on the left are responses to 514 and 654 nm stimuli of 40 msec duration, 100 μm diameter, and of intensity about 1 log unit below saturation. On the right the same two responses are superimposed. *B*, responses of the same rod to stimuli having the same wave-length and intensities but a larger diameter of 750 μm. On the right these two responses are also superimposed.

At low stimulus intensities the responses to different spectral stimuli usually did not superimpose. Text-fig. 11 shows computer-averaged responses to stimuli of 750 μm diameter at wave-lengths of 514 and 680 nm. Each response reached the same peak amplitude of 0·7 mV. The response to 680 nm light hyperpolarized earlier and more rapidly than that elicited by the 514 nm light. Schwartz (1975*b*) reported this earlier component and concluded that it results from cone excitation. Based upon the time

course and spectral sensitivity of the early component, we also conclude that it results from a cone input to the rod response.

To what extent does this cone input influence the rod response? A cone component was not found in all rods, but appeared in about 70 % of the 40 rods examined. Even when it was clearly present, however, as in Text-fig. 11, responses to the two wave-lengths showed no significant difference

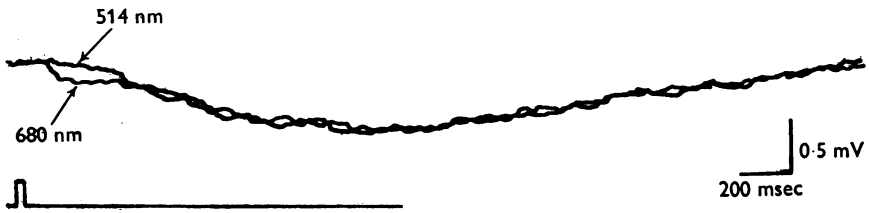

Text-fig. 11. Responses in the rod's linear response range which illustrate a cone contribution. Each superimposed tracing was obtained by computer-averaging of ten responses. Stimuli were 30 msec flashes of 750 μm diameter which delivered 0·05 and 48 quanta/μm^2 at the respective wave-lengths of 514 and 680 nm. These relative intensities, which are shown to elicit equal peak amplitudes of the response, closely approximate the requirements for equal quantum catches by the rod photopigment. The long wave-length stimulus also elicits a small earlier peak on the rising phase of the response.

in peak amplitude, provided that stimulus intensities were adjusted to ensure equal quantum catches by the rod photopigment. Thus the cone component had no significant effect upon peak amplitude of the rod's response. In every rod that exhibited a cone component, higher stimulus intensities evoked a much larger rod component having a shorter latency and reduced time-to-peak. Thus at higher stimulus intensities the rod component of the response very effectively masked the cone component, as shown in Text-fig. 10.

Our results on the spectral sensitivity of the rod response differ from those of Schwartz (1975*b*), who reported that with large, weak stimuli the sensitivity of rods at wave-lengths above 620 nm is greater than predicted from the absorption spectrum of the rod photopigment. For all measurements in this paper we maintained the retina in a fully dark-adapted state. When the retina was deliberately light adapted the relative size of the rod component decreased with respect to the cone component, undoubtedly because of the well known selective desensitization of rods by light adaptation. We thus suggest that the greater long-wave-length sensitivity reported by Schwartz resulted from his working with a more light-adapted retina. This explanation is consistent with his lower reported maximum values of quantal sensitivity.

In summary, in a dark-adapted rod the peak amplitude of the response, over the range from 0·5 mV to saturation, is determined only by the quantity of light absorbed in rods. The rod response wave form is also uninfluenced by cones at stimulus wave-lengths below about 620 nm. With wave-lengths greater than 620 nm, and with weak stimuli, cones may be seen to interact summatively with about 70 % of the rods. When this occurs the cones contribute a relatively small initial component of the rod response. At all but the lowest stimulus intensities the rod response becomes so large, and its time-to-peak so short, that the cone component becomes completely masked. Under these conditions the cone component, if present, is relatively too small to make any significant contribution to the rod response. The Discussion that follows will thus be restricted to rod–rod interactions.

DISCUSSION

Our results indicate that rods of the snapping turtle are functionally interdependent, the hyperpolarizing light response of any given rod being enhanced by light absorption in neighbouring rods. This effect is referred to as *summative interaction*, which is shown to influence both the time course and the amplitude of rod responses. Our results indicate that under weak, full-field illumination only about 4 % of the recorded response results from light absorbed in the outer segment of the impaled rod, the remainder resulting from the activity of neighbouring rods. Thus a rod should hyperpolarize in response to light absorbed in neighbouring rods, even though it absorbs no light itself, as recently confirmed for rods of the marine toad (Fain, 1975). In snapping turtle each rod interacts summatively with other rods as far distant as 150 μm. On the basis of our measurements of receptor size, and the observation of Underwood (1970) that 40 % of the snapping turtle's photoreceptors are rods, we estimate that each rod could interact summatively with up to 200 rods.

In turtle cones (Baylor *et al.* 1971) and mudpuppy bipolar cells (Werblin & Dowling, 1969), delayed antagonistic effects of the surround caused the responses to larger stimuli to become relatively less polarized than those elicited by smaller stimuli. This was reflected in a crossing of the response wave forms at some point in their time courses. In the cone case this antagonism proved especially sensitive to hypoxia. We have been careful to keep our preparations well oxygenated and we readily observe antagonistic interactions when recording from cones. A notable feature of our dark-adapted rod responses to stimuli of different diameters, however, was that their wave forms intersected tangentially, but never crossed, as they decayed from the peak towards the resting potential. This is seen clearly

in Text-fig. 4. We take this to imply an absence of any delayed antagonism from the surround regions of the rod's receptive field.

Quantal sensitivity

In the Results our measurements of receptor sensitivity were expressed as the flash sensitivity, defined as the change in potential produced in a rod when one photon per square micrometre is delivered to the retina. Of interest is the *quantal sensitivity*, defined as the potential generated by a single photoisomerization in each illuminated rod. Because of interspecies differences in the dimensions of rods, and hence in their optical collecting areas, the quantal sensitivity provides a more meaningful basis for comparison with other species.

Dividing the flash sensitivity by the effective collecting area (13·6 μm^2, see Methods) reveals that for a stimulus 25 μm in diameter, rods in snapping turtle have an average quantal sensitivity of 28 ± 5 (S.E. of mean) μV per photoisomerization per rod. While this value is uncorrected for scattered light, the appropriate correction is likely to be small provided that coupling between the impaled rod and its nearer neighbours is reasonably efficient. Upon enlarging the stimulus to a diameter of 300 μm, so that rods throughout the receptive field would each absorb an average of one effective photon, the response of the typical rod increased to 720 ± 120 (S.E. of mean) μV per photoisomerization per rod. Thus summative interaction can increase the rod's quantal sensitivity by a factor of about 26.

Our value of quantal sensitivity measured with a stimulus of 300 μm diameter is close to the 642 μV per photoisomerization per rod obtained in *Bufo marinus* under similar full-field illumination (Fain, 1975). By contrast, Schwartz (1975*b*) calculated the maximum quantal sensitivity of snapping turtle rods to be 200 μV per photoisomerization per rod. In the red-eared turtle, *Pseudemys scripta*, Baylor & Hodgkin (1973) found their most sensitive rods to have a quantal sensitivity of 130 μV per photoisomerization per rod. They noted a wide variation in measured values, however, and suggested that this was probably due to inconsistency in the state of adaptation of their retinae.

In the present study the quantal sensitivity of any individual rod could be reduced from around 700 μV per photoisomerization per rod to 200 μV per photoisomerization per rod by applying a continuously illuminated background field to the retina (485 nm interference filter, 3·3 quanta sec^{-1} μm^{-2}). With such a background the time-to-peak of the rod response was shortened from 1·6 to about 0·6 sec, typical of the rod responses described by Schwartz. This suggests that the retinae used by Schwartz were not completely dark adapted, and that his estimate of quantal sensitivity does not represent the maximum obtainable in the snapping turtle.

The quantal sensitivity of our red-sensitive cones also varied with stimulus diameter. Since cone sizes are very similar in snapping turtle and red-eared turtle, we took the effective collecting area to be 10 μm^2, as calculated by Baylor & Hodgkin (1973). With a stimulus of 25 μm diameter we found the average quantal sensitivity to be 3·8 μV per photoisomerization per cone, rising to 17·5 μV per photoisomerization per cone, a factor of 4·6, as the stimulus was enlarged to 120 μm in diameter. Our *average* value of 17·5 μV is only slightly lower than the *maximum* quantal sensitivity of 25 μV per photoisomerization per cone obtained by Baylor & Hodgkin (1973) when using stimuli greater than 100 μm in diameter. Our high average sensitivity may have resulted partly from rigorous dark adaptation. Also, since our primary objective was to record from rods, we used only very dim stimuli during micro-electrode penetrations of the retina. While such stimuli seemed adequate for all rods, they may have elicited observable responses from only the most sensitive cones.

The pathway of interaction

In the red-eared turtle, the horizontal cell mediates long-range antagonistic interactions between cones (Baylor *et al.* 1971). Since horizontal cells have only been shown to mediate antagonistic interactions between receptors, and since the receptive fields of horizontal cells proved much larger than those of rods, it seems unlikely that horizontal cells are involved in the summative interactions between rods. Short-range summative interactions between cones have been shown, in the red-eared turtle, to be mediated by direct connexions between cones (Baylor *et al.* 1971). It is thus likely that some form of direct contact between rods forms the anatomical basis for summative rod interactions.

It is an attractive possibility that the long basal processes extending from the synaptic terminal of the snapping turtle rod might contact other rods and mediate summative interactions with them. The nature of such contacts is open to speculation. There is a precedent for interreceptor communication that is mediated chemically via receptor basal processes in the guinea-pig retina (Sjöstrand, 1958). On the other hand, probable electrical coupling through gap junctions at the contact points of such processes has been reported in the carp retina (Witkovsky, Shakib & Ripps, 1974). In snapping turtle the rod basal processes exhibit both *en passage* and terminal swellings. These swellings are intriguing because of their general resemblance to the synaptic boutons found in the vertebrate central nervous system, which contain dense aggregations of mitochondria and synaptic vesicles (Palay, 1956). Thus the swellings on the rod basal processes could be presynaptic specializations at chemical synapses. The detailed pathway of rod interaction in the snapping turtle, and the nature

of the coupling mechanism, must be clarified by further anatomical and physiological studies. Our present work is directed toward those goals.

We wish to express our sincere thanks to Professor Kenneth T. Brown for his assistance and encouragement throughout this work. We gratefully acknowledge the technical assistance of Mr Stephen K. Brown and Ms Gail Smith. Thanks are also due to Drs Denis A. Baylor, Juan I. Korenbrot, Sheldon S. Miller and Roy H. Steinberg for reading earlier drafts of this paper, and to Professor Alan Hodgkin for many helpful comments. The work was supported by U.S.P.H.S. post-doctoral fellowships EY 52502 (DRC) and EY 50414 (WGO), and by U.S.P.H.S. research grant EY 00468 to Professor Brown.

APPENDIX

Previous discussions of light scatter within the retina have been predicated upon the assumption that the scattered intensity distribution of a narrow light beam at the level of the photoreceptors is Gaussian in form (Baylor *et al.* 1971; Schwartz, 1973). In the treatment that follows it will be shown that this assumption is inappropriate for the retina, which consists of large transparent cells whose refractive index is only slightly higher than the medium in which they are suspended. In this Appendix we shall attempt to assess, as realistically as possible, the scattering properties of the turtle retina, while avoiding any arbitrary assumptions concerning the form of the scattered intensity function.

A reliable analysis of retinal light scatter must be related to empirical measurements made in a living preparation. Such measurements can be made by recording from a single photoreceptor *if* it is known to be free of interactions with other photoreceptors. We did not find such a cell in the snapping turtle. However, recordings were made from an isolated cone in a closely related species, the red-eared turtle, *Pseudemys scripta elegans*, by Baylor & Hodgkin (1973). They determined the scattered intensity distribution produced at the level of the receptors by a stimulus of nominal diameter 7 μm. They also measured the unscattered intensity distribution across that stimulus. Analytically, the scattered intensity distribution at the photoreceptors is the convolution of the unscattered intensity distribution of the stimulus with the scattered intensity function of the retina, the scattered intensity function being analogous to the point-spread function of an optical imaging system. The scattered intensity function of the retina of the red-eared turtle is thus defined implicitly by these measurements. Because of the close structural similarity between the two retinae, we believe it can be applied with confidence to the retina of the snapping turtle. Our problem was to determine its form. By applying scattering theory to an idealized retina we were able to generate a scattered intensity function consistent with the intensity distribution measured by Baylor &

Hodgkin (1973) and, in the process, to gain some insight into the mechanisms of retinal light scatter.

Mie (1908) applied the electromagnetic theory to the scattering of a plane monochromatic wave by homogeneous spheres of any given diameter and composition, randomly distributed in a homogeneous medium. An approximation to the Mie theory, which satisfactorily describes scattering at small angles, and which greatly simplifies the calculations, was proposed by Hodkinson & Greenleaves (1963). They assumed the scattered intensity to arise from three sources: (*a*) Fraunhofer diffraction at the boundaries of the spheres, (*b*) refraction of light transmitted through the spheres and (*c*) specular reflexion of light from the spheres' surfaces. The scattered intensity function is calculated by summing the contributions from each of the scattering sources. Scattering by diffraction is dependent upon the size of the spheres but independent of their refractive index. Scattering by refraction depends upon the sphere's refractive index but not upon their dimensions. Scattering by reflexion is negligible in the case of the retina.

We applied this approximation to an idealized retina in which retinal cells were assumed to be approximately spherical and to have a refractive index of 1·40. This is the value for rod outer segments and is likely to be an upper limit (Sidman, 1957). The cells were assumed to be suspended in a medium of refractive index 1·334, the value for physiological saline. To simplify calculations, we considered scattering to occur at a plane 200 μm in front of the receptors, this being the maximum distance of cell bodies from receptor outer segments.

When light was assumed to be scattered by cellular structures of approximately equal size, we were unable to generate any function which, in convolution with the intensity distribution of Baylor's & Hodgkin's stimulus, successfully predicted the scattered distribution of light 'seen' by their isolated cone. It was necessary, instead, to assume light to be scattered with an efficiency of 1·0 by a population of cell structures having an average diameter of 8 μm and also, with an efficiency of 0·5, by a second population of cell structures having an average diameter of 1·5 μm. The actual values of these diameters are, of course, influenced by other assumptions that have been made. The necessity of assuming scattering by structures of at least two different sizes, however, seems realistic in view of the existence of both nuclear and plexiform layers in the retina.

The scattered intensity function calculated on this basis is shown in Text-fig. 12. The central peak of the distribution, which is primarily due to diffraction scattering by the larger retinal structures has a width of 14 μm at the half-maximum points and is well fitted by a Gaussian curve of standard deviation 6 μm (thick dashed line). The calculated function differs from the Gaussian in that it exhibits prominent *skirts* which extend

to a radius of 125 μm. These skirts are due to refraction by all of the retinal structures and to diffraction by the smaller of them. It is clear from this difference that calculations of the light intensity at the receptor level based upon an assumption of Gaussian scattering are likely to be significantly in error for radii greater than about 10 μm.

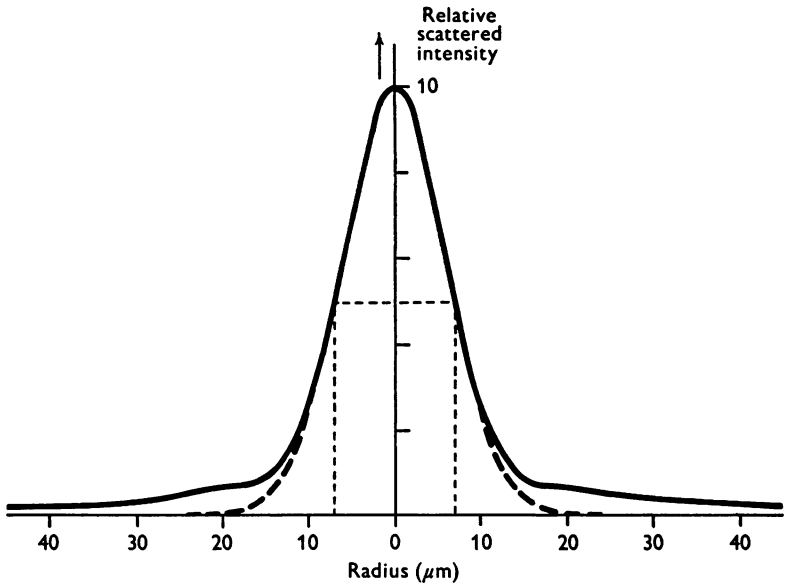

Text-fig. 12. The scattered intensity function of the turtle retina (continuous line) derived by the method described in the Appendix. The central maximum has a width of 14 μm at the half-maximum points. The thick dashed line is a plot of the Gaussian distribution (σ = 6 μm) that best fits the central maximum of the calculated function.

The dashed line in Text-fig. 13 shows the intensity distribution measured by Baylor & Hodgkin (1973) with the isolated cone. Note that it is skewed about the vertical axis. As a basis for comparison the mean of the two sides of the measured distribution was calculated and is plotted as the continuous line. The points were then calculated by convolution of our scattered intensity function (Text-fig. 11) with the intensity distribution of the stimulus used by Baylor & Hodgkin (1973). Our calculated points satisfactorily fit the unskewed curve at radii up to 25 μm. At radii between 25 and 125 μm, our points lie consistently above the measured distribution, a discrepancy which is acceptable since we expect the directional sensitivity of the cone to be of consequence as the scattering angle increases (Baylor & Fettiplace, 1975).

A primary goal in determining the scattered intensity function of the turtle retina was to calculate the expected variation in the quantity of

light (I_o) falling upon an impaled cell at the centre of a stimulus of radius a. We did this by performing the integration:

$$I_o = 2\pi \int_o^a F(r) r \, dr,$$

where $F(r)$ is the theoretical scattering function. The results of this are shown in Text-fig. 14. Over the range of stimulus diameters from 25 to 500 μm the curve has a maximum slope of 0·35. Increasing stimulus diameter from 25 to 250 μm while keeping stimulus intensity constant should produce a 2·4-fold increase in the quantity of light scattered on to

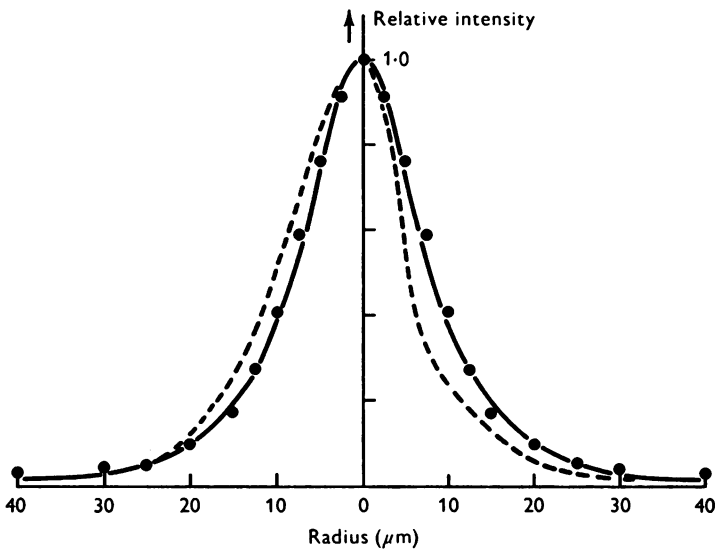

Text-fig. 13. Comparison of calculated and measured light distributions at the photoreceptor layer. The dashed line shows the distribution of light falling upon an isolated turtle cone as a 7 μm diameter stimulus was moved across the retina (after Baylor & Hodgkin, 1973). The continuous line plots the mean of the two sides of this measured distribution. The points were calculated by convolution of the scattered intensity function with the unscattered intensity distribution of the 7 μm diameter stimulus used by Baylor & Hodgkin (1973, fig. 2).

the impaled receptor. Increasing stimulus diameter beyond 250 μm should cause no further increase in this quantity. If rods were isolated from each other, a 2·4-fold increase in the intensity of light falling on an impaled rod would produce a 2·4-fold increase in the measured flash sensitivity. The curve plotted in Text-fig. 8 shows that a 26-fold increase in flash sensitivity was observed experimentally. This strongly suggests that the scattered light alone cannot account for the spatial variation in rod sensitivity and,

more importantly, that the major cause of this variation must be interaction between rods.

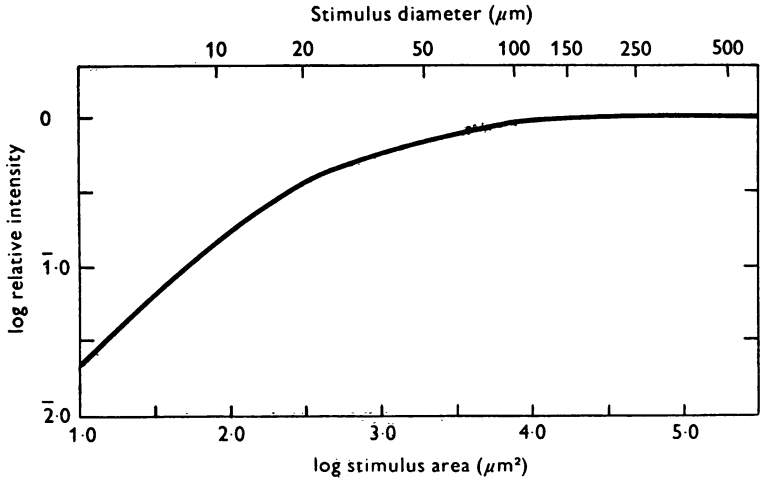

Text-fig. 14. The predicted variation in intensity of light incident upon a single photoreceptor from stimuli of different areas (logarithmic plot). The curve was obtained by integration of the scattered intensity function (see Appendix).

REFERENCES

ARDEN, G. B. & BROWN, K. T. (1965). Some properties of components of the cat electroretinogram revealed by local recording under oil. *J. Physiol.* **176**, 429–461.

BAYLOR, D. A. & FETTIPLACE, R. (1975). Light path and photon capture in turtle photoreceptors. *J. Physiol.* **248**, 433–464.

BAYLOR, D. A. & FUORTES, M. G. F. (1970). Electrical responses of single cones in the retina of the turtle. *J. Physiol.* **207**, 77–92.

BAYLOR, D. A., FUORTES, M. G. F. & O'BRYAN, P. M. (1971). Receptive fields of single cones in the retina of the turtle. *J. Physiol.* **214**, 265–294.

BAYLOR, D. A. & HODGKIN, A. L. (1973). Detection and resolution of visual stimuli by turtle photoreceptors. *J. Physiol.* **234**, 163–198.

BOYNTON, R. M. & WHITTEN, D. N. (1970). Visual adaptation in monkey cones: recordings of late receptor potentials. *Science, N.Y.* **170**, 1423–1426.

BROWN, J. E. & PINTO, L. H. (1974). Ionic mechanism for the photoreceptor potential of the retina of *Bufo marinus*. *J. Physiol.* **236**, 575–591.

BROWN, K. T., WATANABE, K. & MURAKAMI, M. (1965). The early and late receptor potentials of monkey cones and rods. *Cold Spring Harb. Symp. quant. Biol.* **30**, 457–482.

COLES, J. A. & YAMANE, S. (1975). Effects of adapting lights on the time course of the receptor potential of the anuran retinal rod. *J. Physiol.* **247**, 189–207.

COPENHAGEN, D. R. & OWEN, W. G. (1974). Interactions between rods in the turtle retina. *Abstracts of Assoc. for Research in Vision and Ophthal.*, Spring Meeting, p. 14.

DARTNALL, H. J. A. (1972). Photosensitivity. In *Handbook of Sensory Physiology*, **7**, pt. 1, ed. DARTNALL, H. J. A. Heidelberg: Springer-Verlag.

DOWLING, J. E. & RIPPS, H. (1972). Adaptation in skate photoreceptors. *J. gen. Physiol.* **60**, 698.

FAIN, G. L. (1975). Quantum sensitivity of rods in the toad retina. *Science, N.Y.* **187**, 838–841.

FAIN, G. L. & DOWLING, J. E. (1973). Intracellular recordings from single rods and cones in the mudpuppy retina. *Science, N.Y.* **180**, 1178–1181.

GRABOWSKI, S. R. & PAK, W. L. (1975). Intracellular recordings of rod responses during dark-adaptation. *J. Physiol.* **247**, 363–391.

GRABOWSKI, S. R., PINTO, L. H. & PAK, W. L. (1972). Adaptation in retinal rods of axolotl: intracellular recordings. *Science, N.Y.* **176**, 1240–1243.

HODKINSON, J. R. & GREENLEAVES, I. (1963). Computation of light-scattering and extinction by spheres according to diffraction and geometrical optics and some comparisons with the Mie theory. *J. opt. Soc. Am.* **53**, 577–588.

LASANSKY, A. (1971). Synaptic organization of cone cells in the turtle retina. *Phil. Trans. R. Soc.* B **262**, 365–381.

LIEBMAN, P. A. (1972). Microspectrophotometry of photoreceptors. In *Handbook of Sensory Physiology* **7**, pt. 1, ed. DARTNALL, H. J. A. Heidelberg: Springer-Verlag.

MASTERS, J. I. (1954). Some applications in physics of the P-function. *J. Chem. Phys.* **23**, 1865–1874.

MIE, G. (1908). Considerations on the optics of turbid media, especially colloidal metal sols. *Ann. Physik.* **25**, 377.

MUNZ, F. W. & SCHWANZARA, S. A. (1967). A nomogram for retinene$_2$ based visual pigments. *Vision Res.* **7**, 111–120.

NAKA, K. I. & RUSHTON, W. A. H. (1966). S-potentials from luminosity units in the retina of the fish (Cyprinidae). *J. Physiol.* **185**, 587–599.

NORMANN, R. A. & WERBLIN, F. S. (1974). Control of retinal sensitivity. 1. Light and dark adaptation of vertebrate rods and cones. *J. gen. Physiol.* **63**, 137.

O'BRIEN, B. (1951). Vision and resolution in the central retina. *J. opt. Soc. Am.* **41**, 882–894.

PALAY, S. L. (1956). Synapses in the central nervous system. *J. biophys. biochem. Cytol.* **2** (suppl., no. 4, pt. 2), 193–202.

SCHWARTZ, E. A. (1973). Responses of single rods in the retina of the turtle. *J. Physiol.* **232**, 503–514.

SCHWARTZ, E. A. (1975*a*). Rod–rod interaction in the retina of the turtle. *J. Physiol.* **246**, 617–638.

SCHWARTZ, E. A. (1975*b*). Cones excite rods in the retina of the turtle. *J. Physiol.* **246**, 639–651.

SIDMAN, R. L. (1957). The structure and concentration of solids in photoreceptor cells studied by refractometry and interference microscopy. *J. biophys. biochem. Cytol.* **3**, 15–30.

SJÖSTRAND, F. S. (1958). Ultrastructure of retinal rod synapses of the guinea pig eye as revealed by three dimensional reconstructions from serial sections. *J. Ultrastruct. Res.* **2**, 122–170.

UNDERWOOD, G. (1970). The eye. In *Biology of the Reptilia*, chap. 2, ed. GANS, C. & PARSONS, T. S. New York: Academic Press.

WERBLIN, F. S. & DOWLING, J. E. (1969). Organization of the retina of the mudpuppy, *Necturus maculosus*. II. Intracellular recording. *J. Neurophysiol.* **32**, 339–355.

WITKOVSKY, P., SHAKIB, M. & RIPPS, H. (1974). Interreceptoral junctions in the teleost retina. *Investve Ophth.* **13**, 996–1009.

EXPLANATION OF PLATES

PLATE 1

A, photomicrograph of a vertical section through the distal retina of *Chelydra serpentina*. The pigment epithelium has peeled away, revealing the outer segments of the photoreceptors. Cones are easily distinguished from rods by their narrower outer segments and clearly visible oil droplets. Scale mark represents 18 μm.

B, photomicrograph of a vertical section through the whole retina. The normal relation between receptors and the pigment epithelium is illustrated. The total thickness of the retina in this section is about 220 μm. The scale mark represents 35 μm.

PLATE 2

A, photomicrographs of vertical sections through the retina showing two rods from which recordings were made. The rods were injected iontophoretically with the fluorescent dye Procion Yellow M4R. The outer segments are not visible either because they did not fill with dye or because they are obscured by the apical processes of the pigment epithelium. The synaptic terminals lie close to the nuclei of the cells, are broad, and send out many long basal processes. IS, inner segments; ELM, external limiting membrane; N, nucleus; OPL, outer plexiform layer; INL, inner nuclear layer.

B, camera lucida drawings of the basal processes of three rods stained with Procion Yellow. In two cases, processes were followed into adjacent histological sections (lower drawings).

Scale marks in both cases represent 10 μm. Due to the method of preparation of this material some shrinkage may have taken place.

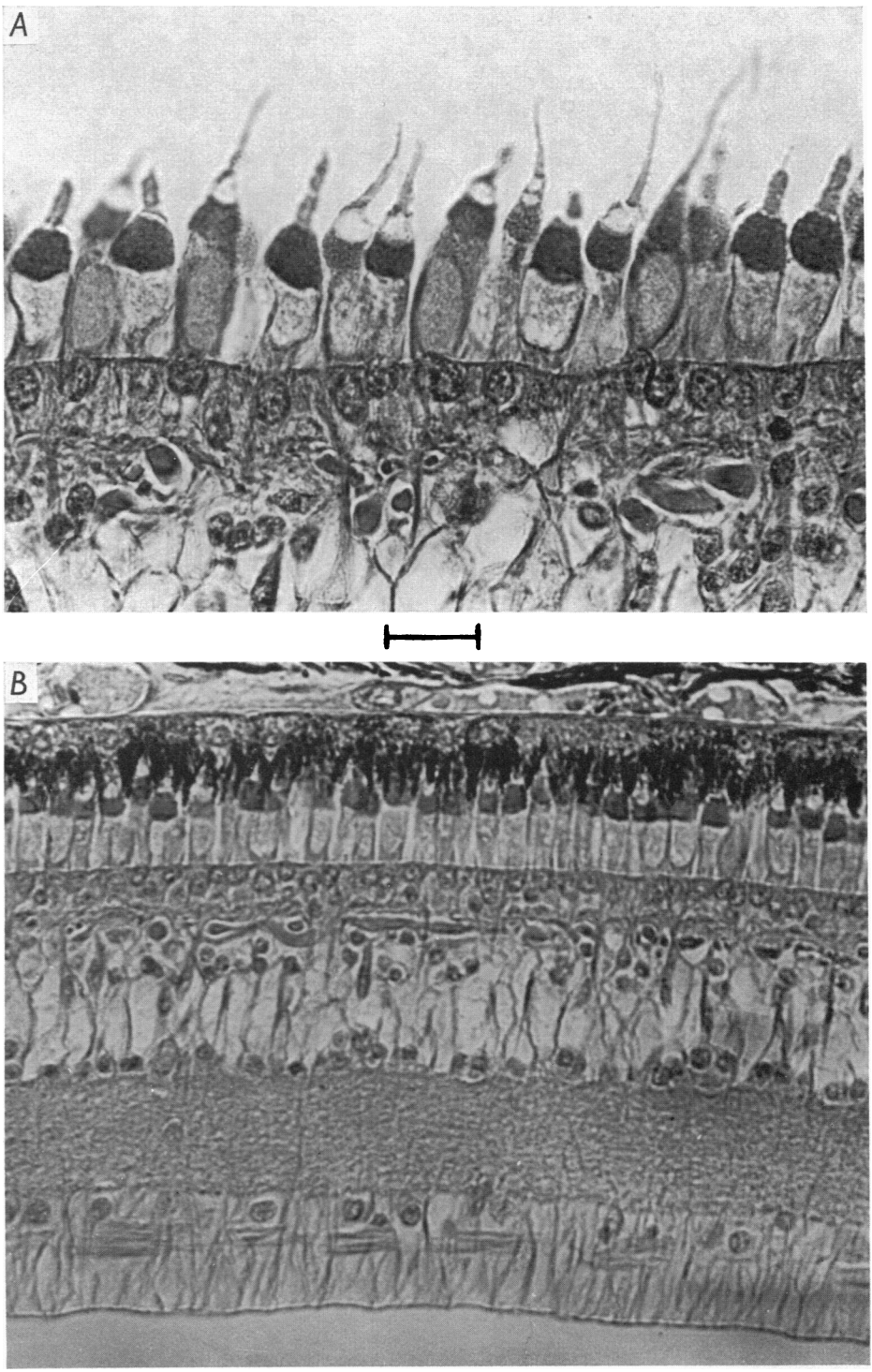
A
B

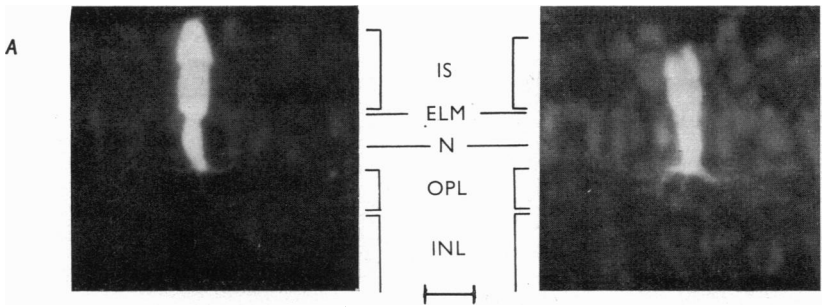
A
IS
ELM
N
OPL
INL

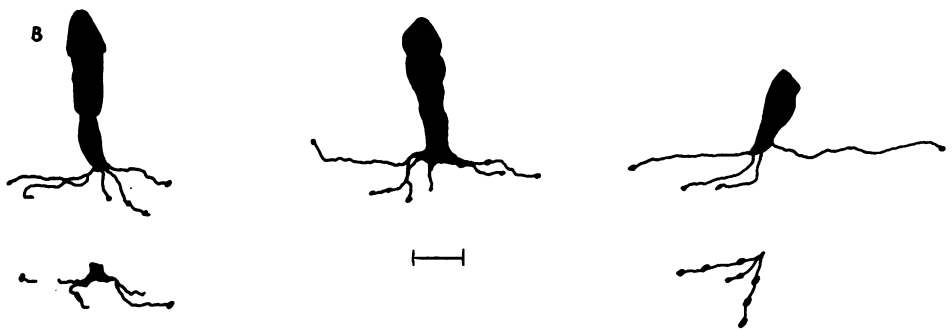
B